Separation of Double-Walled Carbon Nanotubes by Size Exclusion Column Chromatography

Katherine E. Moore,[†,‡] Moritz Pfohl,[‡] Frank Hennrich,[‡] Venkata Sai K. Chakradhanula,[‡,⊥] Christian Kuebel,[‡,⊥,∥] Manfred M. Kappes,[‡,§] Joe G. Shapter,[†] Ralph Krupke,[‡] and Benjamin S. Flavel[‡,*]

[†]Centre for Nanoscale Science and Technology, School of Chemical and Physical Sciences, Flinders University, 5000, Adelaide, Australia, [‡]Institute of Nanotechnology, Karlsruhe Institute of Technology, 76344, Eggenstein-Leopoldshafen, Germany, [§]Institute of Physical Chemistry, Karlsruhe Institute of Technology, 76128, Karlsruhe, Germany, [⊥]Helmholtz Institute Ulm Electrochemical Energy Storage, 89081 Ulm, Germany, and [∥]Karlsruhe Nano Micro Facility, Karlsruhe Institute of Technology, 76344 Eggenstein-Leopoldshafen, Germany

ABSTRACT In this report we demonstrate the separation of raw carbon nanotube material into fractions of double-walled (DWCNTs) and single-walled carbon nanotubes (SWCNTs). Our method utilizes size exclusion chromatography with Sephacryl gel S-200 and yielded two distinct fractions of single- and double-walled nanotubes with average diameters of 0.93 ± 0.03 and 1.64 ± 0.15 nm, respectively. The presented technique is easily scalable and offers an alternative to traditional density gradient ultracentrifugation methods. CNT fractions were characterized by atomic force microscopy and Raman and absorption spectroscopy as well as transmission electron microscopy.

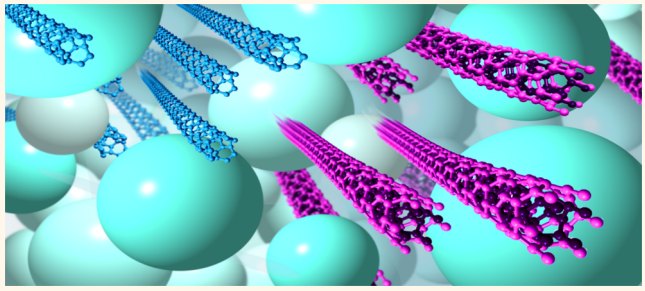

KEYWORDS: carbon nanotube · double · separation · sorting · purification · Sephacryl gel

Double-walled carbon nanotubes (DWCNTs) are a unique intermediate between single-walled carbon nanotubes (SWCNTs) and multiwalled carbon nanotubes (MWCNTs) and are therefore of fundamental interest to the carbon nanotube community. Due to the extraordinary electronic, physical, and optical properties of SWCNTs, a myriad of SWCNT integrated devices for sensing applications can be found in the literature.[1−3] However, for the development of advanced biosensors the integration of a biosensitive element is often necessary. Of course biomodification can be achieved through noncovalent functionalization, such as the wrapping of SWCNTs with DNA,[4,5] or the incorporation of molecules within the surfactant shell,[6] but sometimes it is also desirable to have covalent functionalization avenues available. In this regard, the use of SWCNTs becomes difficult due to degradation of their electronic properties from covalent modification, where disruption of the pristine sp^2-hybridized network is a requirement.[7] DWCNTs offer a unique solution to this problem, where covalent modification can be performed on an outer-wall nanotube only with the inner-wall nanotube remaining pristine and available for signal transduction.[8]

In order to realize this application or indeed alternatives such as field effect transistors[9,10] or atomic force microscopy (AFM) tips,[11] the ability to prepare highly pure DWCNTs is a requirement. Despite research efforts to develop growth processes that favor DWCNT formation, unwanted SWCNTs are still found to be present in the raw material.[12,13] Research efforts have therefore been directed toward methods to isolate and purify DWCNTs. One very successful method was pioneered by Hersam and co-workers in 2009.[14] Their process utilized density gradient ultracentrifugation (DGU) to separate surfactant-wrapped CNTs by their number of walls upon exploiting differences in the buoyant density. In 2010, Huh *et al.* utilized this method to not only separate DWCNTs but also isolate narrow length distributions.[15] This was done by altering both the density gradient and the vertical starting position of

* Address correspondence to benjamin.flavel@kit.edu, www.int.kit.edu/flavel.

Received for review February 7, 2014 and accepted June 4, 2014.

Published online June 04, 2014
10.1021/nn500756a

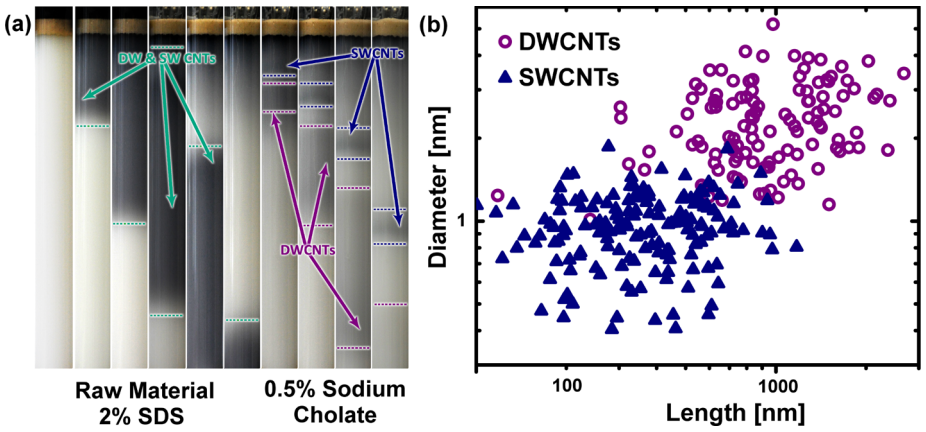

Figure 1. (a) Time-lapse photography (1 h) of the introduction of raw unsorted DWCNT material to the S-200 gel column for the separation of DWCNTs from SWCNTs and (b) diameter *vs* length of SWCNTs and DWCNTs as determined by AFM.

the unsorted material, creating a substantially greater than average density of the dispersed DWCNTs, thus exploiting the length-dependent translation of the nanotubes in response to applied centrifugation. They also reported the first hint of DWCNT separation according to the electronic character of the outer nanotube through the use of cosurfactants at different concentrations throughout the gradient medium. Hersam and co-workers later reported the preparation of high-quality semiconducting and metallic DWCNT fractions in 2011, by conducting sequential DGU, resulting in controlled separation of DWCNTs according to outer-shell electronic character.[16] They achieved very high outer-wall nanotube purity with reports of 96% and 98% for sorted semiconducting and metallic DWCNTs, respectively. While DGU has demonstrated very high quality separation, for many research groups without an ultracentrifuge or the technical expertise in the preparation of intricate density gradients, the preparation of high-purity DWCNT material remains unachievable. For this reason the development of alternative preparation methods is still of fundamental interest.

In this work we describe the use of Sephacryl gel column chromatography to separate SWCNTs from DWCNTs. The use of Sephacryl gel chromatography, developed by Moshammer *et al*. in 2009,[17] has already been shown to be extremely successful in the preparation of SWCNT suspensions. This method allows for the high-throughput separation of metallic (m-) from semiconducting (s-) SWCNTs and in some cases, even enriches zigzag and (*n*, 0) species.[18] The work of Liu *et al*.,[19] Tvrdy *et al*.,[20] and our group[21,22] has then further developed this technique to afford highly pure single-chirality suspensions. It is therefore a logical extension to apply Sephacryl gel techniques to DWCNTs.

RESULTS AND DISCUSSION

As outlined in the Methods section, 125 mL of a 2 wt % sodium dodecyl sulfate (SDS) in H_2O suspension of as-prepared DWCNT material was sonicated for 8 h at 15 °C to yield the raw DWCNT starting solution. This solution was then applied to an S-200 Sephacryl gel bed and washed through with further 2 wt % SDS with the "flow-through" material collected. Figure 1a shows time-lapse photographs of the Sephacryl gel column before addition of the starting material and at various times after addition. Despite a significant portion of the raw material passing through the column, a small fraction remained adsorbed to the gel at the top of the column (absorption spectra of raw and flow-through material can also be found in Figure S1 of the Supporting Information). This is consistent with the previous work of Blanch *et al*.[23] and Flavel *et al*.,[22] who have shown that for HiPco SWCNTs in relatively high SDS concentrations (1.6−2 wt %), only a small amount of the overall nanotube population is adsorbed to the gel, compared to relatively low SDS concentrations (0.4−0.8 wt %). This "flow-through" band is highlighted in green in Figure 1a. Upon addition of 0.5 wt % sodium cholate (SC), the adsorbed CNTs were then eluted from the gel column. This is consistent with previous work,[17] where surfactant exchange results in a reduced interaction of the nanotubes with the gel and subsequent elution. During elution the previously adsorbed DWCNTs and SWCNTs are observed to separate into two distinct bands that are highlighted purple and blue in Figure 1a, respectively. As can be seen in Figure 1a, the DWCNTs travel faster through the S-200 gel compared to the SWCNTs and therefore elute first from the column. Furthermore, the initially tight band of DWCNTs is found to spread out as it passes through the column, whereas the SWCNTs remain roughly confined in a band of the similar size. Despite the extensive use of Sephacryl S-200 size exclusion gel in the separation of SWCNTs,[19−22] the exact mechanism remains under discussion. This is highlighted in the recent work of Tvrdy *et al*.,[20] who identify the separation process of SWCNTs as a selective adsorption and not the expected size exclusion chromatographic (SEC) process, which would have retention time

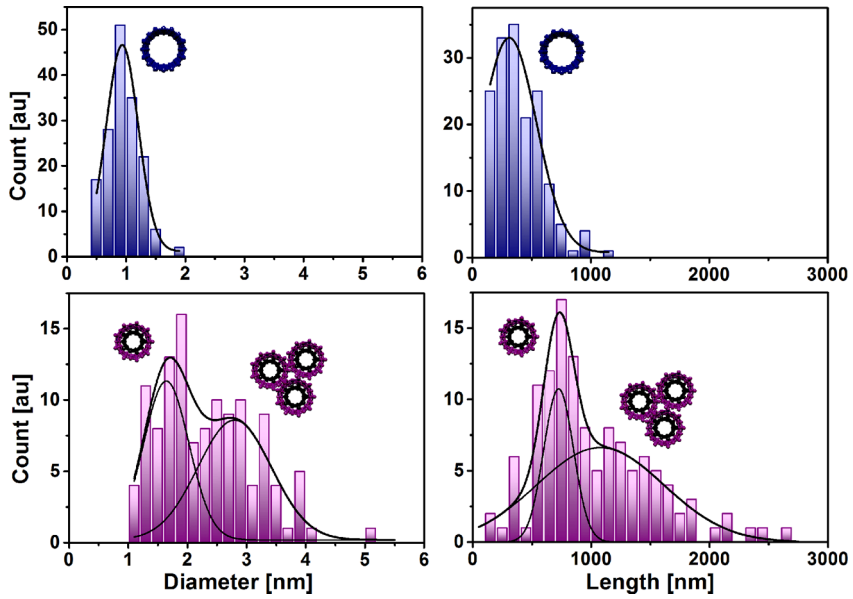

Figure 2. Diameter and length populations determined by AFM of sorted SWCNTs (top) and DWCNTs (bottom) with a Gaussian fit to indicate contribution from individually dispersed tubes and bundles.

dependence. We believe our work to be consistent with the adsorption mechanism proposed by Tvrdy *et al.*; however in the case of the DWCNTs it could be suggested that the spreading of the DWCNT band is due to a size-selective interaction on the gel. Absorption spectra of sequential fractions for the DWCNT and SWCNT material can be found in Figures S2 and S3. Upon inspection of Figure S2, it can be seen that only the leading edge of the "DWCNT band" contains a high content of DWCNTs, with a decrease in both the concentration and optical properites for later fractions. AFM investigation of the DWCNT sample for later fractions is shown in Figure S4 of the Supporting Information, in this case, the fraction labeled "Fraction 5" of the "DWCNTs band". It can be seen that there are indeed CNTs present with an average diameter of 1.05 ± 0.02 nm, which is therefore suggestive of SWCNTs. These SWCNTs have an average length of 910 ± 11 nm, similar to that of the DWCNT sample, which is discussed below. However, as there are no SWCNTs visible in the absorption measurement of "Fraction 5", we believe that they must be highly defected. In absorption measurements we see only a low concentration of DWCNTs, indicating that this nonedge band of DWCNTs is a combination of DWCNTs and defected SWCNTs. It is also important to note at this point that in the near-edge band of DWCNTs (used for all subsequent experiments) no SWCNT material was found by AFM or transmission electron microscopy (TEM). Hence in this case it is the separation of pristine DWCNTs from defected material with reduced adsorption properties that is observed, rather than size exclusion within the DWCNT population.

Likewise the clear separation of the SWCNT and DWCNT bands could also be due to size-dependent retention times on the gel. In Figure 2, AFM measurements comparing the SWCNT and DWCNT fractions are shown (representative AFM images can be seen in Figure S5 of the Supporting Information). In the case of the SWCNTs, a Gaussian can be fitted to the histograms of both the diameter and length with an average diameter of 0.93 ± 0.03 nm and average length of 310 ± 28 nm. It is apparent that the SWCNT sample consisted predominantly of individually dispersed nanotubes, without the presence of large bundles. In the case of DWCNTs, however, there are clearly two subpopulations for both diameter and length distributions, corresponding to individually dispersed DWCNTs and bundles. The increased affinity for DWCNTs to form bundles compared to SWCNTs is believed to be due to the significantly longer tube length and increased diameter, which would lead to increased van der Waals interactions.[24,25] The average diameter and length of the individually dispersed DWCNTs is 1.64 ± 0.15 nm and 725 ± 250 nm, respectively. A further observation from AFM is that the average diameter of the DWCNTs is larger than that of the SWCNTs by 0.71 nm, very close to twice the literature value of the intertube distance (3.44 Å),[26] indicating that the SWCNTs are approximately equivalent to the size of the inner tubes of DWCNTs. It is therefore possible that the presence of SWCNTs has origins in sonication-induced exfoliation of DWCNTs, as well as being present in the raw material.[12,13]

It is well known that raw DWCNT material contains not only small-diameter SWCNTs but also large-diameter SWCNTs and MWCNTs. Indeed it is therefore entirely possible that the additional peak that we have attributed to bundled DWCNT material could simply be attributed to MWCNTs or large-diameter SWCNTs. The only way to verify this is with TEM measurements. From TEM measurements we were unable to locate any MWCNTs in either the SWCNT or DWCNT fractions.

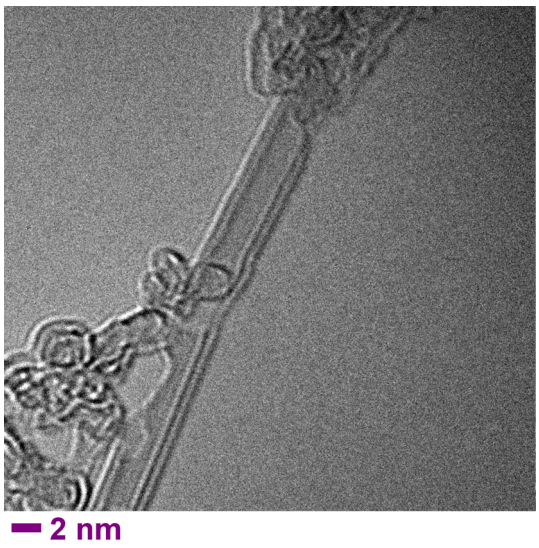

Figure 3. HRTEM micrograph of an individual DWCNT with an outer diameter of 1.7 nm.

Of course this does not rule out the possibility of their existence in either of the fractions due to TEM providing only a limited overview of the entire sample population. However, we note that as we did not see any MWCNTs in TEM, it is unlikely that MWCNTs are present in a high enough concentration to afford the second peak in the AFM diameter distribution of DWCNTs. It is therefore more likely bundling of DWCNTs. A representative TEM image of the DWCNT material can be found in Figure 3, where a free suspended DWCNT can clearly be seen. Furthermore, additional TEM of DWCNT films/bundles can also be found in Figure S5 of the Supporting Information. TEM has also allowed us to determine the location of any large-diameter SWCNTs after the separation process. Within the DWCNT material we were unable to locate any large-diameter SWCNTs; however they were found to be present in the small-diameter SWCNT fraction. This is shown in Figure S6 of the Supporting Information, where two SWCNTs with a diameter of ~2 nm can be seen.

The observation of DWCNTs being longer than the SWCNTs initially appears to be in disagreement with our recent work[22] and the proposed selective cutting mechanism of Hennrich *et al.*[27] and Heller *et al.*,[28] who suggested smaller diameter CNTs are cut to a lesser extent by sonication compared to those with larger diameters. The DWCNTs have a much longer tube length, over twice that of the SWCNTs. From a purely diameter-dependent perspective it would be expected that the DWCNTs (larger diameter) would be shorter than the SWCNTs (small diameter). However, we note that all previous work was performed purely on SWCNTs, and it is unclear what role an additional carbon inner core may play in aiding stability during sonication. Furthermore, in the work of Hersam *et al.*[14] DWCNTs were also found to be ~44% longer than their SWCNT counterparts.

Despite discussions on the cutting mechanism being dependent on wall number, the separation of these two species of CNTs by gel filtration is in agreement with Heller *et al.*,[28] who prepared length- and diameter-separated SWCNTs using both gel electrophoresis and column chromatography. They proposed the mobility of CNTs through the gel matrix to be largely length dependent, as it contributes to the majority of size differences in nanotubes. This is certainly true in this case and is highlighted in Figure 1b; it suggests that the sonication process is of vital importance to enable SEC of DWCNTs. In this work, the raw material contained both SWCNTs and DWCNTs produced in the same CVD synthesis, thus producing tubes of comparable defect contribution. If we make the assumption that the initial length of both tube types is the same, then the longer length of the DWCNTs can be attributed solely to the introduction of a secondary wall, which provides increased structural stability. If we do not assume that the initial length of both tube types is the same, then it may not necessarily be true that the DWCNTs are more stable and shortened at a slower rate. Unfortunately AFM of the raw material cannot be used to determine the initial tube lengths, as it contains a complex mixture of both SWCNTs and DWCNTs, as well as other carbonaceous material that is removed from the sample during separation. Thus, lengths determined from the raw material would not be an accurate representation of the enriched DWCNT and SWCNT samples collected. However, one must consider the mechanics of sonication-induced scission. Initially the nanotubes experience a certain strain force, which makes it unstable in the ultrasonic environment and scission occurs. This continues to occur until the strain force is below the critical value for nanotube disruption and the tube can no longer be shortened.[27] In this work the nanotubes were probe tip sonicated for 8 h, which is a considerable amount of time in such a disruptive environment. We speculate that after this time the CNTs are very close to reaching this critical value, essentially the minimum length, if they have not already. Thus, the rate of scission is unimportant, as given enough time, the nanotubes will reach their minimum length regardless. In this case, it is then only the value of the critical strain force that is relevant, which is determined by the initial size of the nanotubes, determined by tube diameter, initial length, or the number of tube walls. Irrespective of the initial size of the nanotube populations, after sonication there are two very distinct subpopulations, namely, DWCNTs and SWCNTs. If simply the difference in nanotube size was responsible for the separation observed in this work, one would also expect that the same result would be achievable for raw DWCNT material suspended in sodium cholate applied to an S-200 gel column. As a control we have performed this experiment and note that no separation of DWCNTs from SWCNTs is observed. This is summarized in

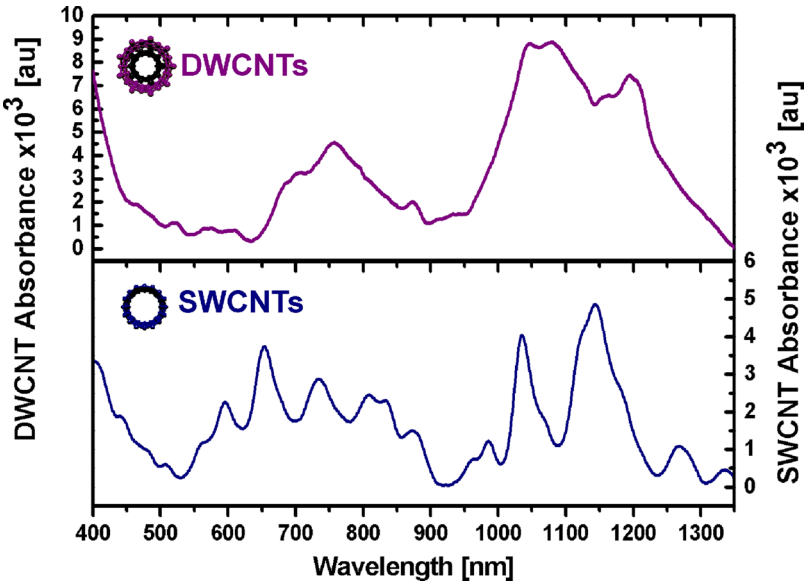

Figure 4. Absorption spectra of the resulting SWCNT and DWCNT fractions in 2 wt % sodium cholate solution. For ease of comparison, the DWCNT spectrum has been subtracted. Details of the background subtraction process can be found in Figure S8 of the Supporting Information.

Figure S7 of the Supporting Information. This tends to suggest that despite the DWCNT and SWCNT fractions having very different size distributions, the mechanism is not a simple size exclusion process. A likely explanation is that once CNTs become trapped on a Sephacryl gel column in SDS, it is the large-diameter CNTs that are first solubilized by sodium cholate with the small-diameter CNTs eluting last. In this case we certainly have two distinctly different diameter regimes, and the true mechanism is likely a combination of diameter-dependent solvation by sodium cholate and length-dependent size exclusion.

The collected SWCNT and DWCNT fractions were then analyzed by absorption spectroscopy. Figure 4 shows typical spectra of SWCNT and DWCNT suspensions in 0.5 wt % sodium cholate. The SWCNT spectra can be divided into two distinct regions, namely, 900−1250 nm and 550−900 nm, which correspond to the first (S_{11}) and second (S_{22}) optical transition of SWCNTs, respectively, and are in agreement with literature for small-diameter HiPco process prepared SWCNTs.[19−22] With the use of data from Weisman and co-workers,[29] this corresponds to CNT diameters of ∼0.8−1.2 nm and is in agreement with our AFM measurements. Likewise the DWCNTs can also be divided into two regions; however, compared to SWCNTs, the peaks in the region of 950−1250 nm are distinctly broader. While this region most likely consists of some S_{11} transitions due to the presence of smaller diameter inner-wall nanotubes, this region is predominately dominated by the S_{22} optical transitions of large-diameter outer-wall nanotubes with ∼1.5−2 nm diameter. The region 500−900 nm then consists of a mixture of S_{22} transitions of inner-wall nanotubes and S_{33} transitions of outer-wall nanotubes. Due to the strong absorption of water above 1400 nm, it was not possible to probe S_{11} transitions of the DWCNT fraction in solution (without the use of D_2O). Therefore, we prepared thin films of DWCNTs and SWCNTs on glass substrates *via* vacuum filtration.[30] These thin films in the dry state allowed us to perform absorption spectroscopy of the DWCNT and SWCNT fractions up to 2500 nm, as shown in Figure 5 (solid lines). Here it is important to remember that thin film measurements cannot be directly compared to solution measurements (highly dispersed CNTs) due to the excitonic properties of nanotubes being greatly affected by many-body interactions, Coulomb interaction, and charge transfer between adjacent nanotubes in bundles (thin CNT films). However, the presence of a clear S_{11} absorption (1600−2200 nm) can be seen for the DWCNTs that is not seen for SWCNTs. This large broad peak is a superposition of many carbon nanotube diameters ranging from 1.5 to 2 nm and is consistent with solution measurements.

The use of CNT thin films also allowed us to further verify the presence of DWCNT and SWCNT fractions *via* a method outlined by Hersam and co-workers[14,16] using thionyl chloride doping.

The treatment of CNT thin films with thionyl chloride has been shown to suppress small band gap optical transitions upon shifting the CNT Fermi level into the HOMO band.[14,16] In this way, the S_{11} and perhaps even some S_{22} transitions (for large-diameter CNTs) appear to be quenched in absorption spectroscopy measurements. Thionyl chloride doping experiments are represented by a dotted line in Figure 5. The broad S_{11} (1600−2200 nm) and S_{22} (900−1250 nm) regions and the S_{11} (900−1250 nm) region were suppressed for the DWCNTs and SWCNTs, respectively, upon thionyl chloride treatment. Interestingly, for the DWCNTs two peaks in the region 900−1250 nm remain after

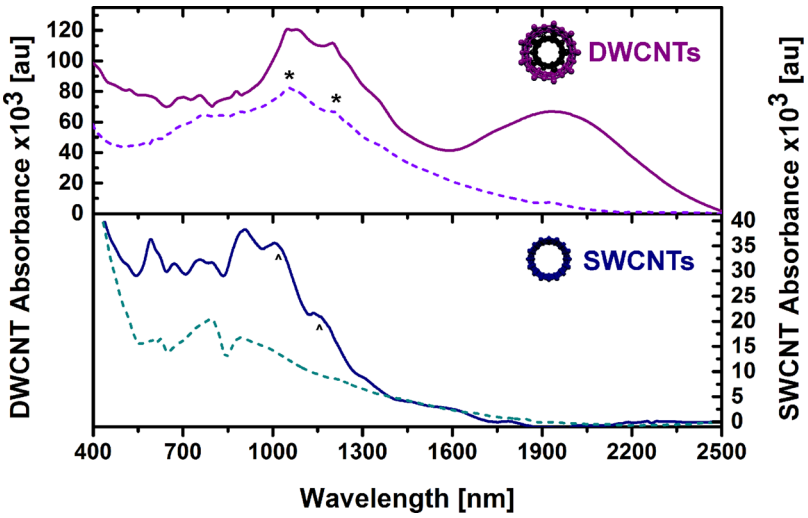

Figure 5. Absorption spectra of sorted DWCNT (top) and SWCNT (bottom) films, before and after treatment with thionyl chloride (solid and dashed line, respectively).

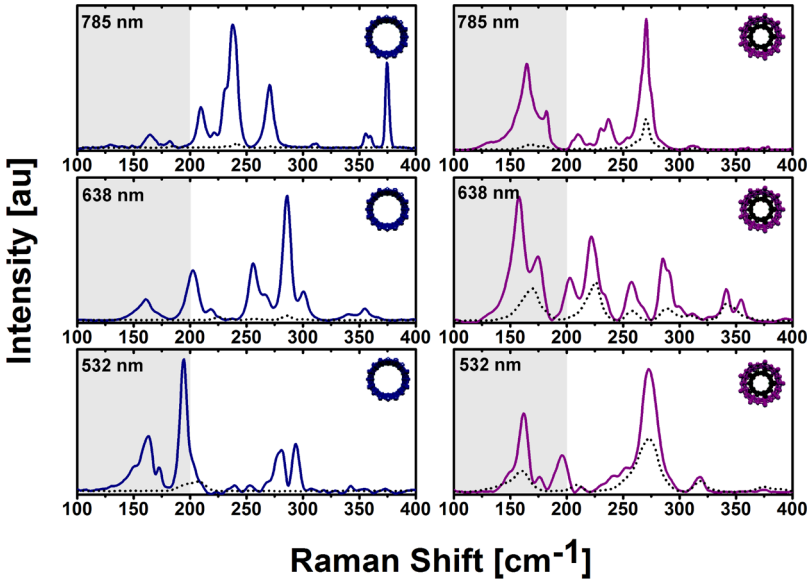

Figure 6. Raman spectra of the radial breathing modes of SWCNTs (left) and DWCNTs (right) with 785, 638, and 532 nm laser excitation before and after treatment with thionyl chloride (solid and dashed lines, respectively).

thionyl chloride doping, which are indicated by asterisks. These peaks are also seen in the SWCNT film (indicated by carats) before doping, and it can clearly be seen that these S_{11} transitions from nanotubes of this diameter are doped by thionyl chloride. The fact that peaks remain in this region for the DWCNT sample can only by explained by the presence of smaller diameter inner-wall SWCNTs. In this case the outer wall has shielded the inner wall from chemical doping by thionyl chloride.

Raman analysis was then further used to analyze the DWCNT and SWCNT thin films. In the work of Hersam and co-workers,[14,16] it was demonstrated that when the CNTs were treated with concentrated sulfuric acid, the exposed outer-wall nanotubes reacted at a significantly faster rate than the inner-wall nanotubes, where the outer wall acts as a protective shield for the inner wall. This was concluded from observing the CNT radial breathing modes (RBM) before and after acid treatment. This experiment has been reproduced in our work and can be seen in Figure S9 of the Supporting Information; however as it is unclear if one is only etching the outer wall, we have opted for a nondestructive approach to demonstrate the effect of inner-tube shielding. In this case, Raman spectra were recorded for each film before and after treatment with thionyl chloride. As mentioned previously, thionyl chloride quenches the small band gap energy transitions, resulting in significant changes in absorption. Figure 6 shows Raman spectra for SWCNTs (left) and DWCNTs (right) at the three different excitation wavelengths of 785, 638, and 532 nm. The use of different wavelengths allows for different diameter tubes to be probed and affords an

accurate representation of the carbon nanotube population. The peak position of the RBM can be used in conjunction with the Kataura plot[31,32] and Weisman data[29] to determine the nanotube chiralities present in each sample and can be seen in the Supporting Information.

Peaks in the shaded region of Figure 6, below 200 cm^{-1}, are a result of excitation of tubes with diameters greater than ~1.2 nm, which in the case of DWNTs correspond to outer-wall tubes. Inversely, the region above 200 cm^{-1} corresponds to tubes with diameters between 0.50 and 1.2 nm. Before treatment, there are an abundance of peaks in each sample; however, there are slightly more peaks in the DWCNT case. This is expected, as the more complex structure of the DWCNTs gives rise to an increased number of nanotube types. Upon looking at the shaded regions of Figure 6, it is also evident that there are more peaks corresponding to large-diameter tubes present in the DWCNT sample. This is particularly apparent in the case of 785 and 638 nm laser excitation. As can be seen at 532 nm excitation, there are large-diameter SW tubes present in the SW fraction, which is confirmed by TEM (see Figure S6 of the Supporting Information). However, they are presumably very low in quantity, as there is not a significant S_{11} absorption visible in the absorption spectra of the film and AFM analysis shows minimal tubes with diameters above 1.4 nm. After thionyl chloride treatment there is a reduction in peak intensity for all SWCNTs peaks with only a few low-intensity peaks remaining at ~195, 290, and 240 cm^{-1} at 532, 638, and 785 nm laser excitation, respectively. However, it is noted that these peaks are reduced in intensity by ~91%, 97%, and 97%, respectively, with all remaining RBMs no longer present. This is expected in the SWCNT case, as all nanotubes are exposed to the thionyl choride chemical environment. A curious feature noted in the Raman measurement of undoped SWCNTs at 785 nm was a peak at 375 cm^{-1} corresponding to the (8,0) nanotube. This tube has a very small diameter of 0.626 nm and can be considered small enough to be contained within a DWCNT. However, after treatment this peak is completely removed, indicating it had been exposed to the thionyl chloride, and hence is a single small-diameter nanotube. Indeed the AFM histogram of SWCNT diameters in Figure 2 shows the presence of a small portion of individualized CNTs with diameters ranging between 0.4 and 0.6 nm. Whether this nanotube was initially present inside a DWCNT and removed *via* sonication remains speculative.

In the case of the DWCNT spectra, the effect of thionyl chloride is much more complex, with many peaks persistent after doping. From the 785 nm laser excitation spectrum, it is clear that the majority of the outer-wall nanotube RBMs, assigned as (15,6), (18,0), and (17,1) have been quenched (shaded region). Conversely, the peak at 270 cm^{-1} (11,0) retained 24% of its original intensity, an indication that this tube has been semiprotected from the doping agent. The 638 nm spectrum shows three clear outer-wall nanotube peaks at ~158 (16,6), 174 (18,0), and 200 cm^{-1} (9,9). These outer-wall nanotube peaks are then once again quenched upon exposure to thionyl chloride. The peaks above 200 cm^{-1} at ~220 (11,5), 258 (11,1), 290 (7,5), and 340 cm^{-1} (6,4) retain 46%, 27%, 24%, and 50% of their peak intensity, respectively, indicating that they are all inner-walled tubes, semiprotected from the thionyl chloride. Lastly, if one considers the spectra at 532 nm, there are two clear peaks associated with outer-wall nanotubes at ~162 (16,5) and 195 cm^{-1} (16,0), which after thionyl chloride treatment are reduced by ~73% and 100%. However, the inner-wall nanotube at ~273 cm^{-1} (12,0) is reduced in intensity by only ~57%. The observation of thionyl chloride to influence both the outer and inner wall (although to a significantly reduced extent) was unexpected by us but points out that the outer-wall shielding is not 100%. This has been observed previously by Kalbac *et al.*, who also observed that chemical doping of the inner tubes was strongly dependent on its electronic character, with metallic inner tubes doped more easily than semiconducting inner tubes.[33] The inner wall is obviously not completely isolated from the outer wall, and it is hence possible to see changes in the surrounding environment in the optical properties of both nanotubes.

CONCLUSION

In this work we have demonstrated the separation of DWCNTs from SWCNTs containing starting material using fast, easily scalable, and financially viable gel column chromatography. It was determined from extensive AFM analysis that the raw DWCNT material contained two CNT populations of distinctly different length and diameter, namely, DWCNTs and SWCNTs. This distinct difference in size may initially lead one to believe that a typical size exclusion process is responsible for the separation of DWCNTs from SWCNTs; however control experiments show that it is more likely a combination of diameter-dependent solvation by sodium cholate and length-dependent size exclusion. Regardless of the mechanism responsible for separation, this work provides a convenient avenue to prepare enriched DWCNTs in a straightforward and easily scalable manner.

METHODS

The DWCNT raw material (average diameter ~2 nm) used in this work was supplied by Unidym, lot no. OE-130807. Suspensions of raw material for size exclusion chromatography were prepared by suspending 50 mg of DWCNT powder in 125 mL of H_2O with 2 wt % of SDS (Sigma-Aldrich) using a tip

sonicator (Bandelin, 200 W maximum power, 20 kHz, in pulsed mode with 100 ms pulses) applied for 8 h at ~20% power. During sonication, the suspension was placed in a 500 mL water bath to dissipate excess heat, without additional cooling. The CNT suspension was then ready to be introduced into the column.

Gel filtration was performed as previously[21] described with only a few changes using S-200 gel filtration medium (Amersham Biosciences) in a glass column 30 cm in length and 2 cm inner diameter. The column was filled with filtration medium and compacted slightly by applying pressure with compressed air to yield a final gel height of ~25 cm. For the separation, ~10 mL of as prepared DWCNT raw material solution was added to the top of the column, and subsequently, a solution of 2 wt % SDS in H_2O was washed through the column under applied pressure to ensure a flow rate of ~1 mL min^{-1}. During this step, single- and double-walled CNTs became trapped on the gel matrix. Once all starting material had been washed through, ~10 mL of 0.5 wt % sodium cholate was added to the column, which subsequently removed the DWCNTs followed by the SWCNTs from the gel medium. These two species were collected as 4 mL fractions for characterization.

Spectroscopic characterization of the sorted material was carried out by UV–vis–NIR spectroscopy and Raman spectroscopy. UV–vis–NIR absorption spectra of the sorted fractions were recorded on a Varian Cary 500 spectrophotometer. Raman absorption spectra were taken with an XploRA confocal microscope (Horiba) with laser energies of 1.58 eV (785 nm), 1.94 eV (638 nm), and 2.33 eV (532 nm) under a 50× objective. Power and gratings were optimized appropriately for each wavelength.

TEM samples were prepared by drop-casting suspensions containing the nanotubes in water onto lacey carbon coated copper grids (Quantifoil GmbH), dried using silica gel. Subsequently they were washed three times followed by drying under a silica gel environment.

SWCNT TEM investigations were performed in a ZEISS Libra 200FE transmission electron microscope operated at 200 kV and equipped with a field emission gun, an in-column filter (Omega-filter), a high-angle annular dark-field (HAADF) detector, and an energy-dispersive X-ray (EDX) spectrometer (SiLi detector, Noran). DWCNT TEM analysis was performed using an image-corrected FEI Titan 80-300 microscope operated at 300 kV and equipped with a Gatan US1000 CCD camera for TEM imaging and electron diffraction. All micrographs were taken with a 4K × 4K CCD camera and analyzed with the software package Digital Micrographs (version 1.71.38, Gatan Company).

Films of the sorted SWCNTs and DWCNTs were prepared by vacuum filtration[30] and then transferred onto clean glass substrates. Treatment of the films with 95–98% sulfuric acid (Sigma-Aldrich) was done by placing a few drops on the film and allowing 10 min for the reaction to occur. After exposure, the excess acid was removed with a pasteur pipet and the CNT sample allowed to dry in air for several days.

Films were doped with $SOCl_2$ (Sigma-Aldrich) by coating the surface with a few drops of $SOCl_2$ and allowing to air-dry for several minutes.

To prepare the AFM samples, 10 μL of CNT solution was spin coated onto 1 × 1 cm^2 clean silicon surfaces (ABC-Gmbh) at 1500 rpm for 1 min, then gently rinsed with H_2O. AFM tapping mode images were taken in ambient conditions with a multimode head and a NanoScope III controller (Digital Instruments) using silicon cantilevers (Mikromasch) with a fundamental resonance frequency between 250 and 400 kHz. Topographic height and phase images were obtained simultaneously with feedback controls optimized for each sample.

Conflict of Interest: The authors declare no competing financial interest.

Acknowledgment. The authors wish to acknowledge and thank Dr. Harald Roesner, of the University of Muenster, for assistance with TEM measrements. The authors also wish to acknowledge Unidym for a sample of their DWCNTs, lot no. OE-130807. K.E.M. appreciatively acknowledges the Australian Nanotechnology Network (ANN), The Playford Memorial Trust, and the Australian Microscopy and Microanalysis Research Facility (AMMRF). K.E.M. also wishes to thank the Cathy Chandler Bursary, the Amy Forwood Trust, BankSA, and Flinders University for overseas traveling scholarships. The authors are grateful to the Karlsruhe Nano Micro Facility (KNMF) for access to the TEM facilities. This research was also supported by the Bundesministerium fur Bildung und Forschung (BMBF) as administered by POF-NanoMicro. B.S.F. gratefully acknowledges support from the Deutsche Forschungsgemeinschaft's Emmy Noether Program under grant number FL 834/1-1.

Supporting Information Available: Extensive spectroscopic (absorption and Raman) and TEM data are available free of charge *via* the Internet at http://pubs.acs.org.

REFERENCES AND NOTES

1. Jin, H.; Heller, D. A.; Kalbacova, M.; Kim, J.-H.; Zhang, J.; Boghossian, A. A.; Maheshri, N.; Strano, M. S. Detection of Single-Molecule H_2O_2 Signalling from Epidermal Growth Factor Receptor Using Fluorescent Single-Walled Carbon Nanotubes. *Nat. Nanotechnol.* **2010**, *5*, 302–309.
2. Khalap, V. R.; Sheps, T.; Kane, A. A.; Collins, P. G. Hydrogen Sensing and Sensitivity of Palladium-Decorated Single-Walled Carbon Nanotubes with Defects. *Nano Lett.* **2010**, *10*, 896–901.
3. Cella, L. N.; Chen, W.; Myung, N. V.; Mulchandani, A. Single-Walled Carbon Nanotube-Based Chemiresistive Affinity Biosensors for Small Molecules: Ultrasensitive Glucose Detection. *J. Am. Chem. Soc.* **2010**, *132*, 5024–5026.
4. Zheng, M.; Jagota, A.; Strano, M. S.; Santos, A. P.; Barone, P.; Chou, S. G.; Diner, B. A.; Dresselhaus, M. S.; Mclean, R. S.; Onoa, G. B.; *et al*. Structure-Based Carbon Nanotube Sorting by Sequence-Dependent DNA Assembly. *Science* **2003**, *302*, 1545–1548.
5. Tu, X.; Manohar, S.; Jagota, A.; Zheng, M. DNA Sequence Motifs for Structure-Specific Recognition and Separation of Carbon Nanotubes. *Nature* **2009**, *460*, 250–253.
6. Roquelet, C.; Lauret, J.-S.; Alain-Rizzo, V.; Voisin, C.; Fleurier, R.; Delarue, M.; Garrot, D.; Loiseau, A.; Roussignol, P.; Delaire, J. A.; *et al*. Π-Stacking Functionalization of Carbon Nanotubes through Micelle Swelling. *ChemPhysChem* **2010**, *11*, 1667–1672.
7. Matsumura, H.; Ando, T. Conductance of Carbon Nanotubes with a Stone-Wales Defect. *J. Phys. Chem. Soc. Jpn.* **2001**, *70*, 2657–2665.
8. Huang, J.; Ng, A. L.; Piao, Y.; Chen, C.-F.; Green, A. A.; Sun, C.-F.; Hersam, M. C.; Lee, C. S.; Wang, Y. Covalently Functionalized Double-Walled Carbon Nanotubes Combine High Sensitivity and Selectivity in the Electrical Detection of Small Molecules. *J. Am. Chem. Soc.* **2013**, *135*, 2306–2312.
9. Ha, B.; Shin, D. H.; Park, J.; Lee, C. J. Electronic Structure and Field Emission Properties of Double-Walled Carbon Nanotubes Synthesized by Hydrogen Arc Discharge. *J. Phys. Chem. C* **2007**, *112*, 430–435.
10. Shimada, T.; Sugai, T.; Ohno, Y.; Kishimoto, S.; Mizutani, T.; Yoshida, H.; Okazaki, T.; Shinohara, H. Double-Wall Carbon Nanotube Field-Effect Transistors: Ambipolar Transport Characteristics. *Appl. Phys. Lett.* **2004**, *84*, 2412–2414.
11. Kuwahara, S.; Akita, S.; Shirakihara, M.; Sugai, T.; Nakayama, Y.; Shinohara, H. Fabrication and Characterization of High-Resolution AFM Tips with High-Quality Double-Wall Carbon Nanotubes. *Chem. Phys. Lett.* **2006**, *429*, 581–585.
12. Lyu, S. C.; Lee, T. J.; Yang, C. W.; Lee, C. J. Synthesis and Characterization of High-Quality Double-Walled Carbon Nanotubes by Catalytic Decomposition of Alcohol. *Chem. Commun.* **2003**, 1404–1405.
13. Yamada, T.; Namai, T.; Hata, K.; Futaba, D. N.; Mizuno, K.; Fan, J.; Yudasaka, M.; Yumura, M.; Iijima, S. Size-Selective Growth of Double-Walled Carbon Nanotube Forests from Engineered Iron Catalysts. *Nat. Nanotechnol.* **2006**, *1*, 131–136.
14. Green, A. A.; Hersam, M. C. Processing and Properties of Highly Enriched Double-Wall Carbon Nanotubes. *Nat. Nanotechnol.* **2009**, *4*, 64–70.
15. Huh, J. Y.; Walker, A. R. H.; Ro, H. W.; Obrzut, J.; Mansfield, E.; Geiss, R.; Fagan, J. A. Separation and Characterization of

Double-Wall Carbon Nanotube Subpopulations. *J. Phys. Chem. C* **2010**, *114*, 11343–11351.
16. Green, A. A.; Hersam, M. C. Properties and Application of Double-Walled Carbon Nanotubes Sorted by Outer-Wall Electronic Type. *ACS Nano* **2011**, *5*, 1459–1467.
17. Moshammer, K.; Hennrich, F.; Kappes, M. Selective Suspension in Aqueous Sodium Dodecyl Sulfate According to Electronic Structure Type Allows Simple Separation of Metallic from Semiconducting Single-Walled Carbon Nanotubes. *Nano Res.* **2009**, *2*, 599–606.
18. Blum, C.; Stürzl, N.; Hennrich, F.; Lebedkin, S.; Heeg, S.; Dumlich, H.; Reich, S.; Kappes, M. M. Selective Bundling of Zigzag Single-Walled Carbon Nanotubes. *ACS Nano* **2011**, *5*, 2847–2854.
19. Liu, H.; Nishide, D.; Tanaka, T.; Kataura, H. Large-Scale Single-Chirality Separation of Single-Wall Carbon Nanotubes by Simple Gel Chromatography. *Nat. Commun.* **2011**, *2*, 309.
20. Tvrdy, K.; Jain, R. M.; Han, R.; Hilmer, A. J.; McNicholas, T. P.; Strano, M. S. A Kinetic Model for the Deterministic Prediction of Gel-Based Single-Chirality Single-Walled Carbon Nanotube Separation. *ACS Nano* **2013**, *7*, 1779–1789.
21. Flavel, B. S.; Kappes, M. M.; Krupke, R.; Hennrich, F. Separation of Single-Walled Carbon Nanotubes by 1-Dodecanol-Mediated Size-Exclusion Chromatography. *ACS Nano* **2013**, *7*, 3557–3564.
22. Flavel, B. S.; Moore, K. E.; Pfohl, M.; Kappes, M. M.; Hennrich, F. Separation of Single-Walled Carbon Nanotubes with a Gel Permeation Chromatography System. *ACS Nano* **2014**, *8*, 1817–1826.
23. Blanch, A. J.; Quinton, J. S.; Shapter, J. G. The Role of Sodium Dodecyl Sulfate Concentration in the Separation of Carbon Nanotubes Using Gel Chromatography. *Carbon* **2013**, *60*, 471–480.
24. Clerk-Maxwell, J. O Ver De Continuiteit Van Den Gas- En Vloeistofiocstand Academisch Proefschrift. *Nature* **1874**, *10*, 477–480.
25. Hiemenz, P. C. *Principles of Colloid and Surface Chemistry*; Marcel Dekker: New York, 1977.
26. Saito, R.; Matsuo, R.; Kimura, T.; Dresselhaus, G.; Dresselhaus, M. S. Anomalous Potential Barrier of Double-Wall Carbon Nanotube. *Chem. Phys. Lett.* **2001**, *348*, 187–193.
27. Hennrich, F.; Krupke, R.; Arnold, K.; Rojas Stütz, J. A.; Lebedkin, S.; Koch, T.; Schimmel, T.; Kappes, M. M. The Mechanism of Cavitation-Induced Scission of Single-Walled Carbon Nanotubes. *J. Phys. Chem. B* **2007**, *111*, 1932–1937.
28. Heller, D. A.; Mayrhofer, R. M.; Baik, S.; Grinkova, Y. V.; Usrey, M. L.; Strano, M. S. Concomitant Length and Diameter Separation of Single-Walled Carbon Nanotubes. *J. Am. Chem. Soc.* **2004**, *126*, 14567–14573.
29. Bachilo, S. M.; Strano, M. S.; Kittrell, C.; Hauge, R. H.; Smalley, R. E.; Weisman, R. B. Structure-Assigned Optical Spectra of Single-Walled Carbon Nanotubes. *Science* **2002**, *298*, 2361–2366.
30. Wu, Z.; Chen, Z.; Du, X.; Logan, J. M.; Sippel, J.; Nikolou, M.; Kamaras, K.; Reynolds, J. R.; Tanner, D. B.; Hebard, A. F.; *et al.* Transparent, Conductive Carbon Nanotube Films. *Science* **2004**, *305*, 1273–1276.
31. Maruyama, S. *Kataura-Plot for Resonant Raman*. http://www.photon.t.u-tokyo.ac.jp/~maruyama/kataura/kataura.html (accessed 07/02/2014).
32. Araujo, P. T.; Doorn, S. K.; Kilina, S.; Tretiak, S.; Einarsson, E.; Maruyama, S.; Chacham, H.; Pimenta, M. A.; Jorio, A. Third and Fourth Optical Transitions in Semiconducting Carbon Nanotubes. *Phys. Rev. Lett.* **2007**, *98*, 067401(1−4).
33. Kalbac, M.; Green, A. A.; Hersam, M. C.; Kavan, L. Tuning of Sorted Double-Walled Carbon Nanotubes by Electrochemical Charging. *ACS Nano* **2010**, *4*, 459–469.